Elastomer
Vol. 38, No. 4, pp 354~362 (2003)

Investigation of Bottom Cracks in the Carbonated Poly(ethylene terephthalate) Bottle

Min-Young Lyu†,*, Youlee Pae, and Changwoon Nah**
ADMS Technology Chungnam, S. KOREA
**Department of Die and Mould Design, Institute of Precision Machinery Technology, Seoul National University of Technology, 172 Gongneung 2-dong, Nowon-gu, Seoul, 139-743, S. KOREA*
***Department of Polymer Science and Technology, School of Advanced Materials Engineering, Chonbuk National University, Chonbuk, S. KOREA*
(Received November 17, 2003, Revised & Accepted December 3, 2003)

ABSTRACT : The use of a petaloid design for the bottom of carbonated poly(ethylene terephthalate)(PET) bottles is widely spread. This study investigated the causes of bottom cracks. The tensile yield stress variations of PET according to the crystallinity and stretch ratio were examined, then the stretch ratio and strength in the bottom area of a blown bottle were analyzed. A crack test was also performed to observe the cracking phenomena. The distribution of the effective stress and maximum principal stress were both examined using computer simulation to seek the influence of the bottom design on crack. It was concluded that the bottom cracks occurred because of inadequate material strength due to the insufficient stretching of PET, plus the coarse design of a petaloid bottom. The stretch ratio at the bottom during bottle blowing should be higher than the strain hardening point of PET to produce enhanced mechanical strength. The cracks in the bottom of the PET bottles occurred through crazing below the yield stress. The maximum principal stress was higher in the valleys of the petaloid bottom than in the rest bottom area, and the maximum principal stress had a strong effect on the cracks.

Keywords : crack, PET bottle, crazing, stretch ratio, maximum principal stress

Ⅰ. Introduction

Poly(ethylene terephthalate) (PET) bottles as beverage containers can be divided into three categories according to the contents of the bottle.[1-6] First, standard bottles for non-pressurized liquids such as water or alcohol, second, carbonated soft drink (CSD) bottles for carbonated liquids, third, hot fillable bottles for fruit juices. The hot fillable bottles should have thermal resistance since the fruit juices are sterilized and then poured into the bottles at elevated temperatures. The CSD bottles should have high mechanical strength compared with the other categories of bottles to resist the high pressure of carbon dioxide gas.

Carbonated bottles had consisted in two pieces, a PET blown bottle and base cup. The PET blown bottle was hemispherical bottom, and the base cup was made of polyethylene (PE). These were then assembled to create a carbonated container. However, since the mid of 1980's these two-piece bottles have been changed to one-piece bottles consisting of only a PET blown bottle without a base cup. The bottom shape of a one-piece bottle for carbonated liquids is petaloid in shape to enable self-standing. This one-piece bottle has advantages compared with the two-piece bottle as it reduces the manufacturing processes and materials by eliminating the bottom

† 대표저자(*e-mail : mylyu@snut.ac.kr*)

supporter, i.e., the base cup. However, problems with cracks have occurred in one-piece bottles in the petaloid bottom. Previous publications on cracks in PET bottle are very limited and mostly deal with the characteristics of the fracturing[7,8] and cracking[9-13] of PET materials. Articles concerning the bottom cracks of PET bottles have appeared in patents.[14-17] These studies were limited to modifications of the stretch blowing process, preform designs, and cracking test methods.

Accordingly this paper presents a basic investigation of the causes of bottom crack in petaloid PET bottles. The physical properties of PET were examined, then the strength, cracking phenomena, and stress concentration in the bottom of the bottle were investigated. Subsequently, guidelines are suggested for blowing and the bottom design of PET bottles to prevent bottom cracks in carbonated petaloid PET bottles.

Ⅱ. Experimental and Simulation

1. Materials and measurement of tensile yield stress

We used PET with different molecular weight, supplied by Samyang Co. (TRIPET® BI). The intrinsic viscosities of the PET were 0.77, 0.80 and 0.83 dl/g.

The tensile yield stresses of PET specimens with various crystallinities were measured on an Instron 4204 at room temperature. Amorphous specimens were prepared by injection molding (BA 750 CD plus, Batenfeld) with quenching the mold at 15℃ water coolant. Subsequently various crystalline specimens were obtained by crystallizing the amorphous specimens in oven (HB-501VL, Han Back Co.) for various times at 130℃. The crystallinity was measured by a densimeter (Daeha Trade Co.). Finally the tensile yield stresses of the various crystallized PET specimens were measured on the Instron 4204 with crosshead speed of 2.8 mm/min.

Amorphous specimens were stretched to various stretch ratios on an Instron 4502 with an isothermal chamber to examine the stretch related material strength. The temperature in the isothermal chamber was maintained at 110℃ which was the same temperature as the bottle blowing process. The stretch speed was 500 mm/min. However this speed did not meet the actual stretching speed in the blowing process as the stretch blowing of the PET preform was performed within a second. After stretching the tensile specimens, they were cooled down to room temperature, then the tensile yield stresses of stretched samples were measured on the Instron 4204 with crosshead speed of 2.8 mm/min at room temperature.

2. Bottle Blowing

The preforms used in blowing process were made by injection molding (XL 500 PET, Husky, 72 cavities). The blowing operations for 1.5 ℓ and 350 mℓ bottles were performed using Sidel's (SBO 10/10) and Sipa's (ECS 800) blowing machines, respectively. As soon as heating the preform by lamps up to 110℃, stretch rod stretched preform axially. Subsequently the preforms were blown using 4 MPa of air pressure. The mold temperature was maintained at 10℃ during the blowing process.

3. Cracking Test

Citric acid and sodium bicarbonate were put into water contained PET bottle to make carbon dioxide gas. The contents of carbon dioxide gas were 4.3, 4.7 and 5.0 in volume percentage. In these cases, the weight concentration of carbon dioxide gas were 8.45, 9.23 and 9.82 g/ ℓ respectively. The bottom part of carbonated PET bottle was immersed in 0.2 wt% of NaOH solution to stimulate crack. Then, the positions where the bubble leaked through crack in the bottom of bottle were checked.

4. Simulation of Stress in Carbonated Bottle

The stresses at the bottom of bottles were quantitatively simulated using commercial software,

Abaqus (Version 5.8-16).

The stresses of bottles were simulated with three different model thicknesses, 0.35, 2.0 and 3.36 mm, with corresponding Young's moduli of 77.6, 173.1 and 1731. kg_f/mm^2, respectively. The same thicknesses were also used in simulations with a Poisson's ratio of 0.36. The thickness represented the average thickness of the sidewall, bottom part and preform. The applied pressures were 0.04 and 0.06 kg_f/mm^2 for bottles with a 4.3 volume percentage of carbon dioxide gas at 20 and 35 ℃, respectively. A 4.3 volume percentage of carbon dioxide gas is common in carbonated beverages.

Ⅲ. Results and Discussion

1. Physical Properties of Material

Variations of tensile yield stresses for the PET of various crystallinity are shown in Figure 1. Yield stress increases as the degree of crystallinity increases. The uniformity of polymer chains and the density of material increase as crystallinity increases, thereby resulting in an enhanced mechanical strength.[18-21] As such a high degree of crystallinity in PET has a beneficial effect on the strength of material. The effect of intrinsic viscosity (IV) between 0.77 and 0.83 dl/g on yield stress was negligible.

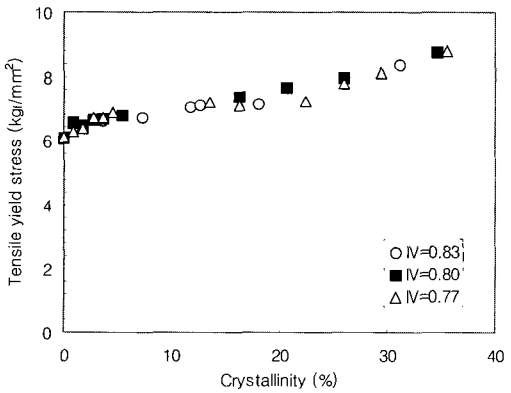

Figure 1. Variations in tensile yield stresses according to crystallinity of PET.

Haze and transmittance could represent degree of transparency of material. Here, the haze increases while the transmittance decreased as crystallinity in PET increases. The thermal crystallinity lowers the transparency of bottle and this is detrimental to the quality of bottle. It has been reported that thermal crystallinity should be lower than 5 % to maintain reasonable quality for a PET bottle.[22] In this range of low crystallinity the tensile strength of PET could not be notably enhanced as shown in Figure 1.

The tensile yield stresses of uniaxially stretched PET are shown in Figure 2. In bottle blowing process preform is stretched biaxially. Thus to create comparable data with biaxial stretching condition, the tensile yield stress was plotted as stretch ratio in thickness direction, i.e., the original thickness to deformed thickness. The stretch ratio in thickness direction in biaxial stretching would be higher than that of uniaxial stretch under the same stretch stress. However this discrepancy was considered to be small and ignored in our discussion. The yield stresses remain at almost the same value for low stretch ratios, between 1 and about 1.7 as shown in Figure 2. However these increase as stretch ratio increases with higher stretch ratios, i.e., higher than 1.7. This behavior of yield stresses in Figure 2 is similar to those of other studies that were performed at elevated temperatures.[1,19,20] During the stretching of PET at elevated temperatures the increment of stress was very small at low stretch ratios.[1,19,20] As

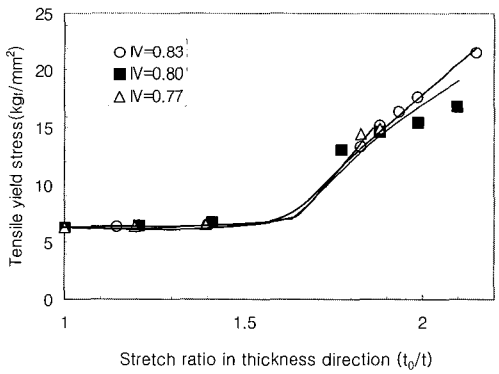

Figure 2. Tensile yield stresses of stretched PET.

stretch ratios increase the molecules are arranged to the stretching direction. Subsequently after certain point of stretch ratio the stress increases drastically as stretch ratio increases. That is the strain hardening of material. Figure 2 shows same physical behavior of strain hardening. Through this examination, we could see that the stretch ratio in bottle blowing should be higher than strain hardening point. The variations of yield stresses according to the stretch ratios for examined IV in our experiment are negligible.

2. Stretch Ratios and Strength of the Bottom of Bottle

The cross sections of preform and blown bottle are shown in Figure 3. We marked points in preform before blowing and than calculated the stretch ratios in thickness direction (thickness ratio of preform to bottle) in blown bottle. Figure 4 and 5 show the profiles of thickness and stretch ratio of feet and valleys in the petaloid bottom of bottles. The thickness near center of bottom is much thicker than that of sidewall of bottle, and the stretch ratio in thickness direction at this center region is near one. The stretch ratio in thickness direction begins to increase after point 5 as shown in Figure 5.

We estimated the tensile strength at each point of bottle by using the stretch ratio in the thickness direction. The relationships among the stretch ratios in blown bottle from preform can be calculated for simplified models as followings.

First of all, if we consider the stretch of sidewall in bottle from preform as shown in Figure 6, the relationship among the stretch ratios in this area would be

$$2\pi R_1 L_1 t_1 = 2\pi R_2 L_2 t_2 \tag{1a}$$

$$\left(t_1/t_2\right) = \left(R_2/R_1\right)\left(L_2/L_1\right) \tag{1b}$$

$$\lambda_t = \lambda_C \lambda_L \tag{1c}$$

where λ_t, λ_C and λ_L are the stretch ratios in thickness, circumferential and longitudinal direction respectively, and are defined as

$$\lambda_t = t_1/t_2,\ \lambda_C = R_2/R_1,\ \lambda_L = L_2/L_1 \tag{2a, 2b, 2c}$$

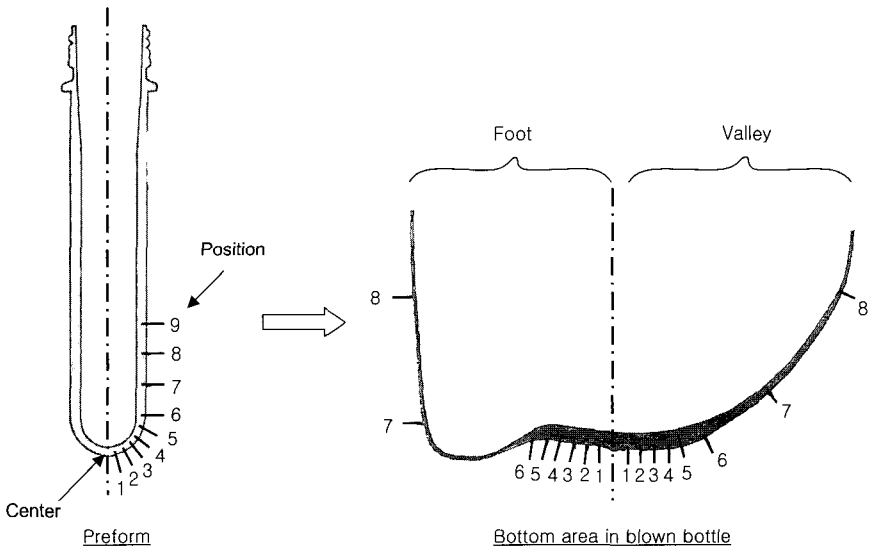

Figure 3. Cross-sections of preform and petaloid bottom of blown bottle.

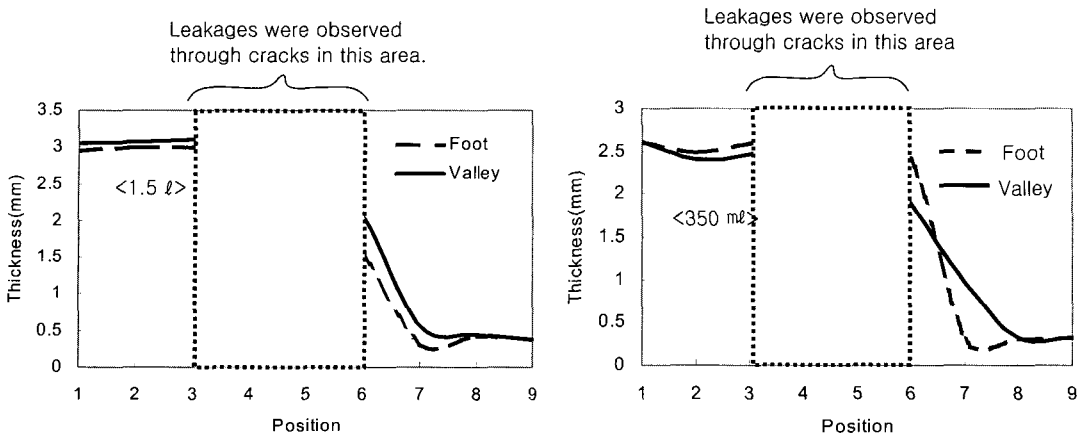

Figure 4. Variations in thicknesses of feet and valleys in petaloid bottom of bottles.

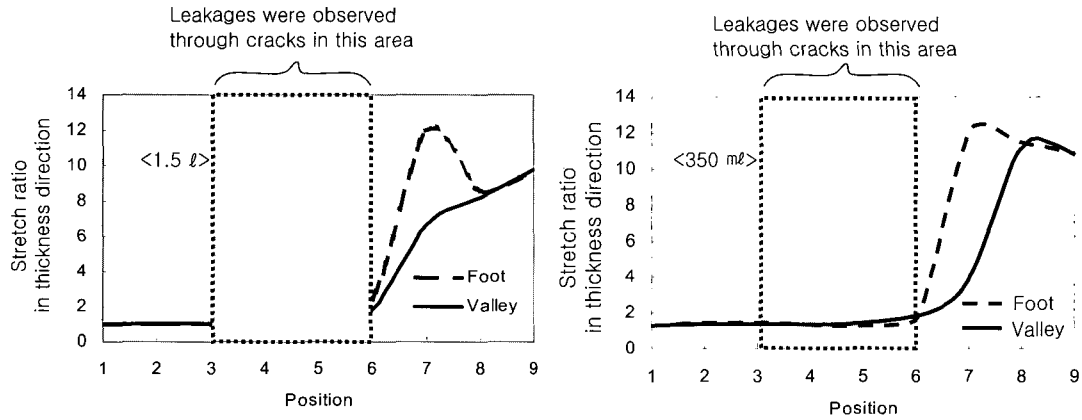

Figure 5. Variations in stretch ratios of feet and valleys in petaloid bottom of bottles.

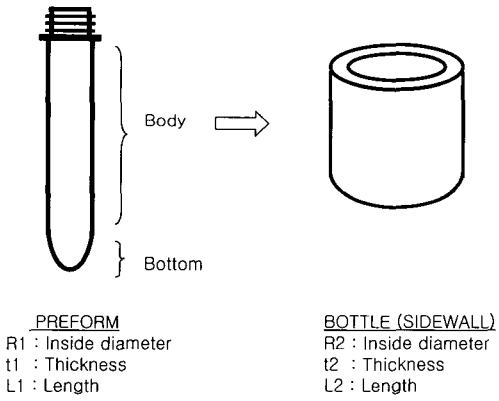

Figure 6. Stretches in sidewall of bottle.

For the stretch ratios in bottom part of bottle, we consider the two simple models as shown Figure 7. The relationships among the stretch ratios when hemisphere of preform becomes hemisphere of bottom in bottle (Figure 7(a)) are

$$2\pi R_1^2 t_1 = 2\pi R_2^2 t_2 \tag{3a}$$

$$\left(t_1/t_2\right) = \left(R_2/R_1\right)^2 \tag{3b}$$

$$\lambda_t = \lambda_C^2 \tag{3c}$$

$$\lambda_C = \lambda_L \tag{3d}$$

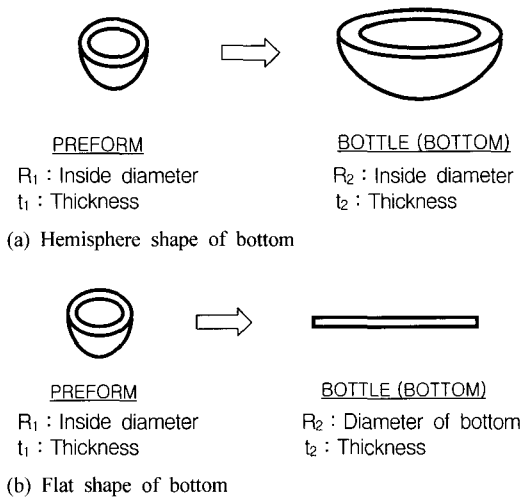

Figure 7. Stretches in bottom of bottle.

If hemisphere of preform becomes flat shape of bottom (Figure 7(b)), the relationships are

$$2\pi R_1^2 t_1 = \pi R_2^2 t_2 \tag{4a}$$

$$\left(t_1/t_2\right) = \left(1/2\right)\left(R_2/R_1\right)^2 \tag{4b}$$

$$\lambda_C = \frac{R_2}{\frac{1}{2}\pi R_1} = \frac{2R_2}{\pi R_1} \tag{4c}$$

$$\therefore \lambda_t = \left(1/2\right)\left(R_2/R_1\right)^2 = \left(\pi^2/8\right)\lambda_C^2 \tag{4d}$$

$$\lambda_C = \lambda_L \tag{4e}$$

We calculated average λ_C using Eqs (3c) and (4d), then estimated the strength in the bottom area of bottle through Figure 2. We simply considered the petaloid bottom was combination of hemispheric and flat shapes. Figure 8 shows estimated yield stress in bottom of bottle. The yield stress increases after point 6 although the stretch ratio begins to increase after point 5. Thus the strength of bottom from point 1 to point 6 are the same. However the thickness of bottom decreases notably from point

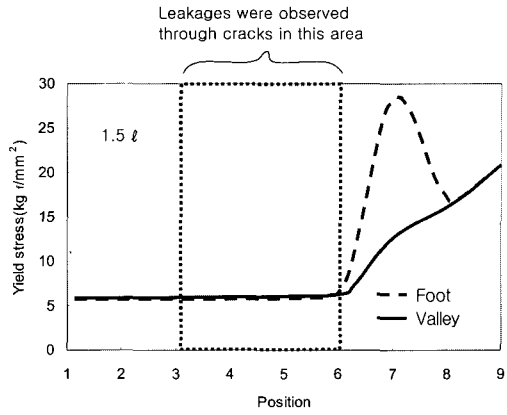

Figure 8. Tensile yield stress in bottom of bottle after blowing operation.

4 or 5 (Figure 4). Through these examinations we can realize structurally weakness of bottom because of abrupt change in thickness between point 4 and 6 without increment of tensile yield stress.

3. Observations of Cracks in Bottle

We observed cracks in the bottom of bottle as shown in Figure 9. There are two directions of cracks. One is the radial crack. In this case, cracks begin bottom center and propagate to outside, radial direction. The radial cracks occurred due to residual stress. The gate in the preform that was manufactured by injection molding was located in the center of bottom. Thus the high thermal residual stress was concentrated near the center of bottom. The other is the circumferential crack. The cracks are located in some distance from the bottom center, and the direction is circumferential. This circumferential cracks occurred due to the stress concentration that was generated by bottom geometry and carbonated gas. The circumferential cracks will be dealt more in next section.

The most cracks that finally made leakage occurred at valley of the petaloid bottom and their directions were circumferential as indicated by arrows in Figure 9. The locations of these cracks were distributed between points 3 and 6 as indicated in Figures 4, 5 and 8. In these points the material

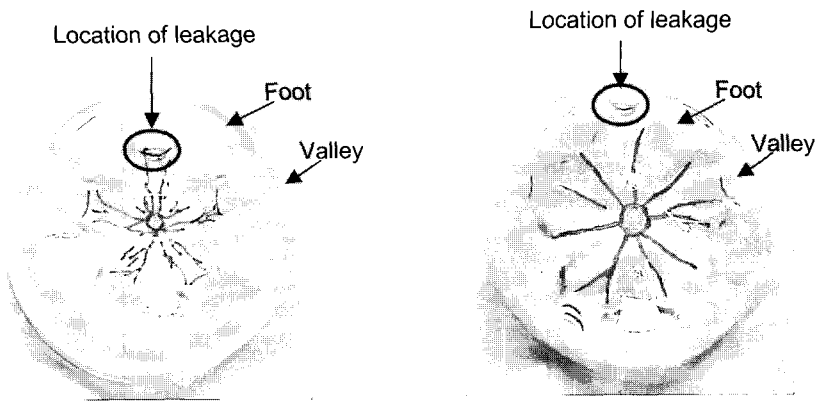

(a) 1.5 ℓ (b) 350 mℓ

Figure 9. Cracks in petaloid bottom of bottle.

strength was low because of insufficient stretching of material as discussed in the previous section.

4. Stresses in Carbonated Bottle

Figure 10 shows the effective stress distribution in bottle for thickness 2.0 mm that was the average thickness of bottom area. The actual thickness in bottle was distributed unevenly. However, we used even thickness in simulation for simple modeling. The objective of this simulation is to investigate the stress distribution that comes from the geometry of petaloid bottom.

The effective stresses (i.e. square root of elastic distortion energy which is being used for criteria of material yielding in von Mises yield criteria[23]) at bottom area are higher than sidewall and the highest effective stresses are distributed at the valleys. This means that the geometrically weakest region is the valley. However the highest effective stresses, 2.13 kg_f/mm^2 in Figure 10 are lower than yield stress of material, 6.3 kgf/mm^2 in Figure 1. Moreover the actual thickness at valley (between point 5 and 5.5 in Figure 4) where the highest effective stress occurred was thicker than model thickness, 2.0 mm. Thus the bottle is safe in these maximum effective stresses. Figure 11 summarizes the maximum effective stress variations according to the thickness of

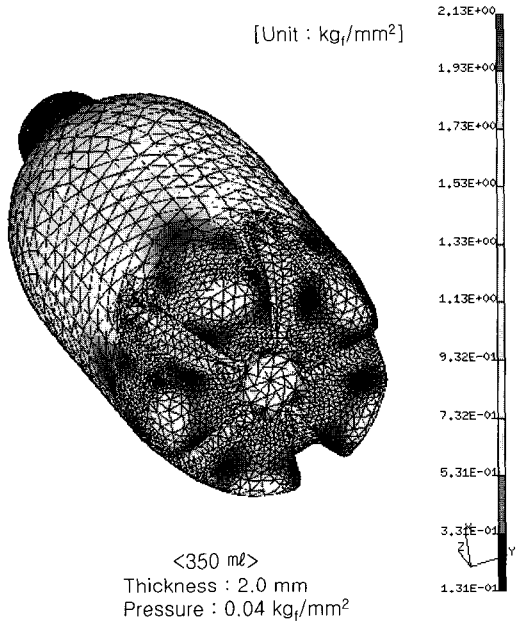

Figure 10. Effective stress distributions in carbonated bottle.

bottom area. As long as bottom thickness is maintained over 2.0 mm, bottle would be safe structurally for stress concentration.

Figure 12 shows the maximum principal stress (i.e. the highest stress among the principal stresses, σ_1, σ_2, and σ_3) in bottle. Crazing occurs in brittle

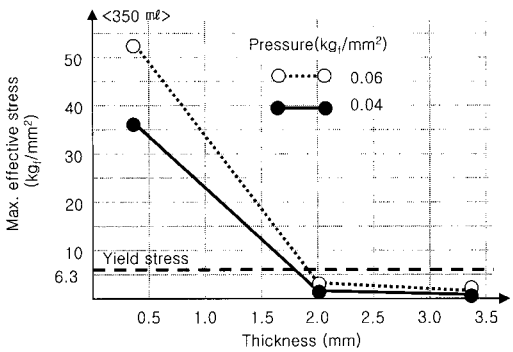

Figure 11. Variations in maximum effective stresses for bottles with different thicknesses.

materials such as amorphous and semi-crystalline polymers under tensile stress.[21,25] And the crazing contour is below the yield contour.[24,25] Crazing is related to tensile stress rather than shear stress.[25,26] Therefore the maximum principal stress is considered important factor for creation of crazing. The highest maximum principal stress of tensile occurs at valleys as shown in Figure 12 (a), and its direction is radial (axial) as shown in Figure 12 (b). This radial direction is perpendicular to the crack direction that made a leakage in bottom as observed in the cracking test. Through these examinations we could see the maximum principal stress among the stresses plays a major role in cracking of bottom in bottle.

Ⅳ. Conclusions

The cracks that resulted in leakage of carbonated liquids in PET bottle occurred in the valleys in the bottom, and their direction was circumferential. The valleys in the petaloid bottom of the bottle exhibited structural weakness and stress, especially maximum principal stress, concentration. These cracks appeared to be related to the crazing associated with the maximum principal stress.

The weak material strength of the bottom of the bottle came from a low stretch ratio that was below the strain hardening point during stretching. The

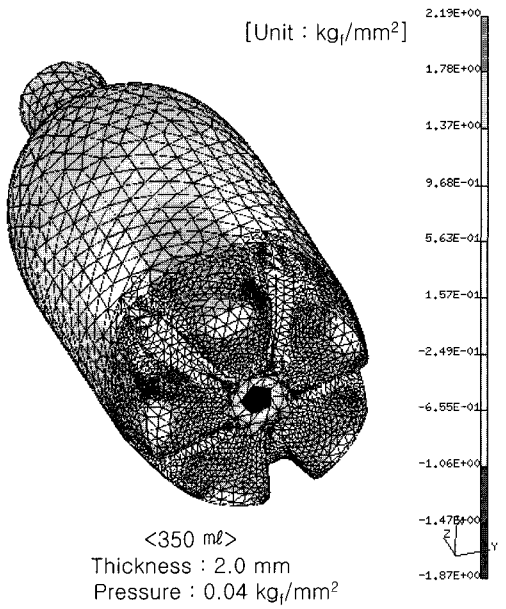

(a) Maximum principal stress distribution

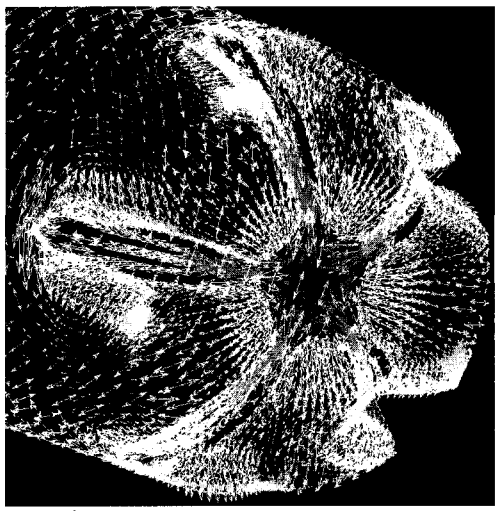

(b) Direction of maximum principal stress

Figure 12. Maximum principal stress distribution and direction.

thickness decreased as the stretch ratio increased without any improvement in the tensile strength with a low stretch ratio. Therefore, stretching in the radial (axial) direction for a petaloid bottom should be increased above the strain hardening point to prevent weakness in the bottom of the bottle. Enhanced strength for the bottom of the bottle can be achieved through increasing the crystallinity with a low stretch ratio. However, thermally induced crystallinity deteriorates the transparency and quality of the bottle.

The highest maximum principal stress occurred in the valleys. The direction of this stress was radial and caused circumferential cracks through crazing. Accordingly, the maximum tensile principal stress should be lowered or minimized in the valleys of a petaloid bottom in a PET bottle to prevent bottom cracks by carbonated liquids.

References

1. C. Bonnebat, G. Roullet and A. J. de Vries, *Polym. Eng. Sci.*, **21**, 189 (1981).
2. L. Erwin, M. A. Pollock and H. Gonzalez, *Polym. Eng. Sci.*, **23**, 826 (1983).
3. M. Cakmak, J. E. Spruiell and J. L. White, *Polym. Eng. Sci.*, **24**, 1390 (1984).
4. M.-Y. Lyu, H. C. Kim, J. S. Lee and H. C. Shin, Conference on the Polymer Society of Korea, **25**(1), 14 (2000).
5. D. Brunnschweiler and J. Hearle, Polyester, The Textile Institute, Manchester, England (1993).
6. H. G de Lorenzi and C. A. Taylor, *Intern. Polym. Process.*, **8**, 365 (1993).
7. J. S. Foot and I. M. Ward, *J. Materials Sci.*, **7**, 367 (1972).
8. V. Tanrattanakul, W. G. Perkins, F. L. Massey, A. Moet, A. Hiltner and E. Baer, *J. Materials Sci.*, **32**, 4749 (1997).
9. J. R. Kastelic and E. Baer, *J. Macromol. Sci.-Phys.*, **B7**(4), 679 (1973).
10. G. Marom, N. Konieczny and M. Mushtakel, *Polymer*, **20**, 1054 (1979).
11. R. P. Kambour, *Polymer Communications*, **25**, 130 (1984).
12. S. A. Jabarin and E. A. Lofgren, *Polym. Eng. Sci.*, **32**, 146 (1992).
13. E. J. Moskala, *Polymer*, **39**, 675 (1998).
14. M. Wider, US Patent 5 009 801 (1991).
15. B. Tekkanat and A. A. Kovacich, B. L. McKinney and W. H. Tiedemann, US Patent 5 001 935 (1991).
16. C. E. Rossio and T. E. Anderson, US Patent 5 073 280 (1991).
17. B. Tekkanat, A. A. Kovacich, B. L. Mckinney and W. H. Tiedemann, US Patent 5 001 935 (1991).
18. J. H. Dumeleton, *J. Polym. Sci.*, **6**, 795 (1968).
19. S. A. Jabarin, *Polym. Eng. Sci.*, **32**, 1341 (1992).
20. F. Rietsch, *Eur. Polym. J.*, **26**, 1077 (1990).
21. T. A. Osswald and G. Menges, "Materials Science of Polymers for Engineers", Hanser, NY (1996).
22. M.-Y. Lyu, H. C. Kim, J. S. Lee and H. C. Shin, *Intern. Polym. Process.*, in press
23. E. G. Thosen C. T. Yang and S. Kobayashi, "Mechanics of Plastic Deformation in Metal Processing", Macmillan, NY(1965).
24. A. M. Donald and E. J. Kramer, *J. Materials Sci.*, **17**, 1871 (1982).
25. N. G. McCrun, C. P. Buckley and C. B. Bucknall, "Principles of Polymer Enginnering", 2nd Ed., Oxford University Press, NY (1997).
26. S. S. Sternstein, L. Ongchin and A. Silverman, *Applied Polymer Symposia*, No. 7, 175 (1968).